research articles Journal of proteome research

Side Chain Chemistry Mediates Backbone Fragmentation in Hydrogen Deficient Peptide Radicals

Qingyu Sun,[†] Hosea Nelson,[‡] Tony Ly,[†] Brian M. Stoltz,*[,‡] and Ryan R. Julian*[,†]

Department of Chemistry, University of California, Riverside, California 92521, and Division of Chemistry and Chemical Engineering, California Institute of Technology, Pasadena, California 91125

Received August 4, 2008

A crown ether based, photolabile radical precursor which forms noncovalent complexes with peptides has been prepared. The peptide/precursor complexes can be electrosprayed, isolated in an ion trap, and then subjected to laser photolysis and collision induced dissociation to generate hydrogen deficient peptide radicals. It is demonstrated that these peptide radicals behave very differently from the hydrogen rich peptide radicals generated by electron capture methods. In fact, it is shown that side chain chemistry dictates both the occurrence and relative abundance of backbone fragments that are observed. Fragmentation at aromatic residues occurs preferentially over most other amino acids. The origin of this selectivity relates to the mechanism by which backbone dissociation is initiated. The first step is abstraction of a β-hydrogen from the side chain, followed by beta-elimination to yield primarily a-type fragment ions. Calculations reveal that those side chains which can easily lose a β-hydrogen correlate well with experimentally favored sites for backbone fragmentation. In addition, radical mediated side chain losses from the parent peptide are frequently observed. Eleven amino acids exhibit unique mass losses from side chains which positively identify that particular amino acid as part of the parent peptide. Therefore, side chain losses allow one to unambiguously narrow the possible sequences for a parent peptide, which when combined with predictable backbone fragmentation should lead to greatly increased confidence in peptide identification.

Keywords: 18-crown-6 ether • photodissociation • iodine • direct dissociation • ultraviolet • proteomics

Introduction

The development of new methods for fragmenting peptides in the gas phase continues to be a major area of interest in order to extend the utility of mass spectrometry (MS). In particular, radical chemistry has received renewed interest following the discovery of electron capture dissociation and electron transfer dissociation (ECD[1] and ETD,[2] respectively), which generate radicals following the addition of an electron to an isolated positively charged even electron ion. The fragmentation obtained by ECD/ETD is desirable, stimulating the investigation of alternative methods for generating radicals on peptides. The most commonly utilized method to date exploits the facile association of many peptides with metal ions.[3−7] Following collisional activation, the metal departs from the peptide to yield a radical species. This method is promising for several reasons: (1) sample preparation is simple, (2) the radical peptide does not need to be covalently modified, and (3) the observed fragmentation of these peptide radicals differs from collision induced dissociation (CID) experiments. On the other hand, this method can be limited by failure of some peptides to ligate with metal ions. In addition, activation of the radical requires substantial heating of the molecule. Alternatively, radical precursors can be covalently installed and then activated by CID.[8−11] Peroxycarbamate, azo, and nitroso functional groups have been successfully employed in this type of experiment, where MS^3 is required to examine fragmentation of the peptide radical. Again, the results can differ substantially from those observed by CID; however, prior chemical modification complicates both sample preparation and analysis of the results, and again activation by CID leads to heating of the molecule prior to generation of the radical.

Recently, we have been developing another approach for generating radicals by photolysis of highly labile radical precursors. For example, iodinated tyrosine residues lose I· exclusively upon absorption of a 266 nm photon, yielding a tyrosyl radical by homolytic cleavage.[12] This chemistry occurs due to the presence of a low lying dissociative excited electronic state, and results in only minimal heating of the remaining molecule. In this manner, a radical can be selectively generated at a specific site in a large molecule, without perturbing the remainder of the molecule. In the case of iodotyrosine, subsequent collisional heating of the radical results in fragmentation at tyrosine and other nearby residues. Similar chemistry has been observed following modification of phosphorylated serine and threonine, which utilizes direct dissociation of a carbon−sulfur bond.[13] However, this methodology has not previously been explored

* To whom correspondence should be addressed. E-mail: (B.M.S.) stoltz@caltech.edu, (R.R.J.) ryan.julian@ucr.edu.
[†] University of California.
[‡] California Institute of Technology.

10.1021/pr800592t CCC: $40.75
Published on Web 12/29/2008

with noncovalently attached radical precursors, which is the subject of the present report.

There are a variety of potential scaffolds for delivering chemical functional groups to peptides via noncovalent interactions.[14−17] Arguably, 18-crown-6 (18C6) is the preferred solution due to its ability to recognize protonated primary amines.[18] Any lysine containing peptide is therefore an excellent host for 18C6, although a protonated N-terminus or even arginine will suffice under mild sampling conditions (particularly if lysine is absent). Therefore, 18C6 can potentially attach to the vast majority of peptides that might be produced by enzymatic digestion in a typical proteomics experiment. In addition, the 18C6 scaffold is amenable to derivatization, yielding lariat crown ethers where a large number of possible functional groups can be attached to the crown. 18C6-based lariat crowns have already been successfully employed to deliver functional groups via noncovalent attachment in previous gas phase experiments with peptides.[14,19] For the present work, it is additionally advantageous that 18C6 does not absorb in the near-ultraviolet and will therefore not interfere with photochemistry carried out in this region.

We have combined the recognition capabilities of 18C6 with a photolabile iodonaphthyl radical precursor in the form of a lariat crown ether. Sample preparation involves simple addition of the lariat crown to the solution containing the peptide. A noncovalent complex then forms which can be efficiently transferred to the gas phase by electrospray ionization. Photoexcitation at 266 nm leads to loss of I·, generating a naphthyl radical which readily abstracts a hydrogen atom from the peptide. Subsequent collisional activation leads to loss of the crown and fragmentation of the radical peptide. It is revealed that dissociation of the peptide is dominated by radical chemistry and surprisingly occurs through strongly favored dissociation channels. In some cases, highly preferential cleavage at aromatic residues is observed. Ab initio calculations suggest that selectivity is controlled by the relative β-hydrogen bond dissociation energies for each amino acid. In addition, prominent side chain losses are observed. Mechanisms for the production of backbone and side chain fragments are proposed, and the utility of side chain losses in peptide identification is explored.

Experimental Methods

5-Iodo-2-naphthoic Acid (1).[20] To a round-bottom flask charged with water (1 mL) and silver sulfate (500 mg, 1.6 mmol, 1.3 equiv) was added sulfuric acid (20 mL). The mixture was allowed to stir and subsequently cooled to room temperature. 2-Naphthoic acid (430 mg, 2.5 mmol, 1 equiv) was added, followed by the addition of iodine (750 mg, 3.0 mmol, 1.15 equiv). The reaction was stirred vigorously at room temperature for 2 h. Carbon tetrachloride (20 mL) was added and the reaction was allowed to stir for an additional hour. The crude reaction mix was slowly added to water (150 mL), and the yellow precipitate was collected by vacuum filtration. The precipitate was taken up in a 10% potassium hydroxide solution (100 mL) and filtered through activated carbon. The resulting colorless solution was acidified to pH 2 with 1 N HCl. The precipitate was recrystalized from EtOAc to yield 200 mg of white crystals.

5-Iodo-2-(2-hydroxymethyl-18-crown-6)-naphthoate (2). To a flame dried 1 dram vial charged with dichloromethane (1.2 mL) was added 5-iodo-2-napthoic acid (74 mg, 0.25 mmol, 1 equiv) and oxalyl chloride (26.4 μL, 0.30 mmol, 1.2 equiv).

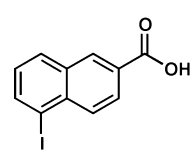

1

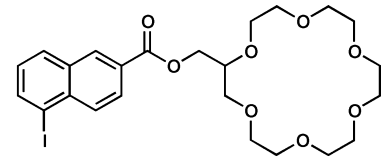

2

The mixture was stirred for 30 min at ambient temperature. A catalytic quantity of DMF (1 μL) was added, and the reaction mixture was stirred for an additional 3 h. The solvent was removed by rotary evaporation to yield the crude acid chloride as a yellow solid. To the crude yellow solid was added dichloromethane (1.2 mL) and 2-hydroxymethyl-18-crown-6 (73.5 mg, 0.25 mmol, 1 equiv), and the reaction mixture was stirred for 30 min at room temperature. Triethylamine (70 μL, 0.30 mmol, 1.2 equiv) was added to the reaction mixture before it was heated to 40 °C for 4 h. The reaction was cooled to room temperature, and condensed by rotary evaporation. Diethyl ether (5 mL) was added, and the resulting suspension was filtered through a celite column. After condensation by rotary evaporation, 115 mg of yellow oil was isolated.

Sample Preparation. Peptides (Ac-AKAKAKAY-OH, AAAYGGFL, AEAEYEK, RGYALG, DRVYIHPF, Ac-ERERERER-NH2, RYLPT, RYLGYL, RPPGFSPFR, AAGMGFFGAR, TRSAW, MEHFRWG, GFQEAYRRFYGPV, RRPWIL, DLWQK, YGGFLRK, KWDNQ, GGYR, YAFEVVG, KKPYIL, SLRRSSCFGGR, AAAKAAA, AAAAKAAAK, EMPFPK, VLPVPQK, AVPYPQR) were purchased from American Peptide Company (Sunnyvale, CA), Quality Controlled Biochemicals (Hopkinton, MA), or Sigma-Aldrich (St. Louis, MO). All chemicals and reagents in this work were used directly without purification unless noted. Sample solutions for electrospray were made by mixing 1 equiv of each peptide stock solution with 4 equiv of iodo-naphthyl crown in 98% acetonitrile to give final concentrations of 10 and 40 μM, respectively.

Mass Spectrometry. A flashlamp-pumped Nd:YAG laser (Continuum Minilite, Santa Clara, CA) was interfaced with the back of an LTQ linear ion trap mass spectrometer (Thermo Electron, San Jose, CA). Fourth-harmonic laser pulses (266 nm) were introduced to the linear ion trap through a quartz window at the posterior of the ion trap. Peptide−crown solutions were infused into a standard electrospray source and transmitted into the linear ion trap. MS^n type experiments (where the first CID step was replaced by photodissociation) were performed on noncovalent peptide−crown complex ions. Laser pulses were synchronized by feeding a TTL trigger signal from the mass spectrometer to the laser via a digital delay generator (Berkeley Nucleonics, San Rafael, CA). All CID steps were employed by applying an excitation voltage on mass-isolated ions using default instrument parameters. Peptide fragments were assigned with the aid of UCSF Protein prospector (http://prospector.ucsf.edu/).

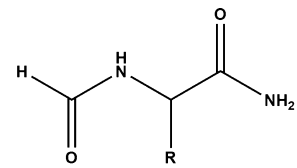

Model Structure for Calculations (R=all amino acid side chains)

Calculations. All *ab initio* calculations were performed at the B3LYP/6−31G(d) level as implemented in Gaussian 03

Version 6.1 Revision D.01. Model peptides (as shown above) were built using Gauss View 3.0. C−H bond dissociation energies (BDEs) for the β-hydrogens of 19 amino acids were obtained by the use of isodesmic reactions, which have been used previously to evaluate α C−H BDEs.[21,22] The reference molecule in each isodesmic reaction was as follows: H-CH_2OH (Ser, Thr), $C_6H_5CH_2$−H (Phe, Trp, His, Tyr), CH_3CH_2−H (Ala), $(CH_3)_2$CH-H (all others).[23] Trans geometry was assumed for all peptides, except for proline, where both conformers were considered. Restricted and unrestricted methods (RB3LYP and UB3LYP) were used on closed-shell and open-shell systems, respectively. Spin contamination was found to be minimal for all systems. The results are in good agreement with previous calculations.[24] The relevant computational numbers for the reference molecules were obtained from the NIST computational standards database.[25]

Results and Discussion

Reagent **2** is designed to complex with peptides in solution via the 18C6 portion of the molecule. The preferred target is lysine; however, under appropriately gentle electrospray conditions, **2** will complex with virtually any protonated peptide. The iodonaphthyl portion of **2** is designed to yield a naphthyl radical following photodissociation of the carbon−iodine bond. Such bonds are known to fragment directly following electronic excitation by ultraviolet radiation.[26] Loss of I· from **2** generates a highly reactive radical in close proximity to a complexed peptide, which can lead to hydrogen abstraction and the generation of a hydrogen deficient peptide radical. To clarify, by hydrogen deficient, we mean a peptide missing a hydrogen relative to the mass of a fully protonated, even electron ion (with no implication for the structure).[27] The hydrogen count distinguishes these radicals from those produced by ECD or ETD, which contain an additional hydrogen relative to a protonated ion. Conveniently, complexes of **2** and the target peptide are created by simply mixing the two reagents and then electrospraying the solution. The addition of crown ethers also has beneficial effects on total ion counts as described previously.[18]

The full mass spectrum generated by electrospray ionization of a solution of **2** and RGYALG is shown in Figure 1a. Abundant adduct formation is observed, in agreement with previous observations. It should be noted that this peptide does not contain lysine, confirming that nonlysine peptides can interact with 18C6 under proper source conditions. Isolation of the peak corresponding to [RGYALG + **2** + H]$^+$ followed by photoactivation at 266 nm is shown in Figure 1b. There are three products observed. Direct dissociation of the carbon iodine bond leads to loss of I· with retention of the noncovalent complex. Simple dissociation of the noncovalent complex is also observed; however, upon closer inspection, it is revealed in the magnified spectrum that a fraction of the protonated peptide has undergone hydrogen abstraction *and* fracture of the noncovalent complex. CID experiments on the peptide radical can be performed by reisolating the directly generated peptide radical shown in Figure 1b; however, it is often simpler to generate the radical peptide by subjecting the noncovalent radical complex to CID as shown in Figure 1c. This pathway typically yields the peptide radical as the primary product. The photodissociation step in these experiments can be conducted on the nanosecond time scale, and the remaining steps are CID experiments, meaning that interrogation of radical peptides

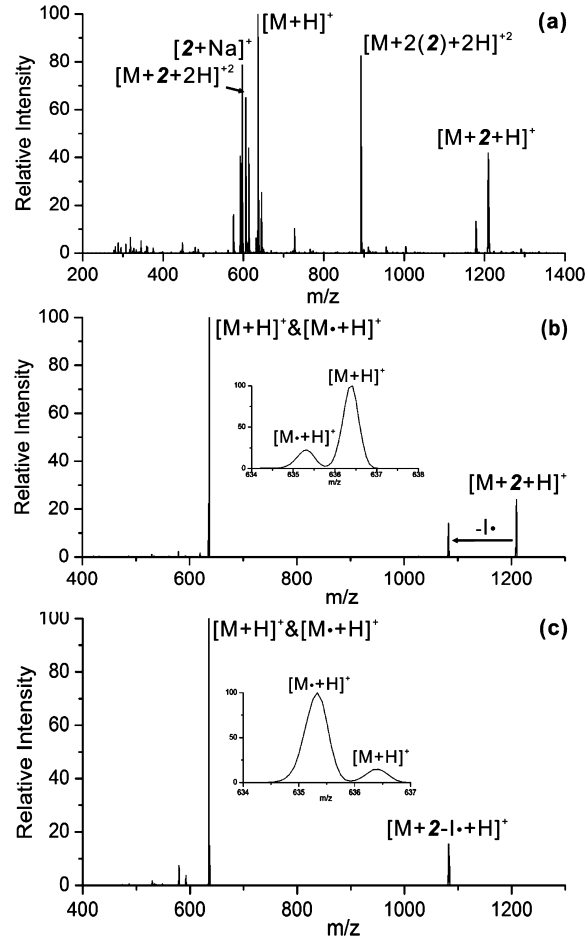

Figure 1. (a) Full mass spectrum of **2** and RGYALG, demonstrating abundant complex formation. (b) Photoactivation at 266 nm leads to generation of a radical complex, and both radical and nonradical peptides. (c) Collisional activation of the radical complex yields primarily radical peptide.

could be performed in tandem with CID experiments on the nonradical form of the peptide, if desired.

Sufficient radical peptide is produced in these experiments to carry out multiple subsequent steps of collisional activation; however, the overall efficiency of the process has not been maximized. The usable radical ion count is frequently only 10−20% of the precursor peptide intensity. It is likely that hydrogen abstraction efficiency is currently limited by three unproductive channels. First, internal conversion of the photon energy can occur and will lead to simple heating of the complex without generating any radicals. Second, any luminescence will similarly lead to unproductive deactivation. It may be possible to reduce these channels through optimization of the chromophore. Third, generation of the radical may be followed by fracture of the noncovalent bond holding the complex together without prior abstraction of hydrogen from the peptide. It is possible that further optimization of the radical delivery agent could reduce this phenomenon; however, the current reagent is well-suited for experiments which are not high-throughput and will suffice to explore the relevant chemistry for potentially interesting fragmentation.

The results obtained by fragmenting [RGYALG• + H]$^+$ are shown in Figure 2a. There is only one major cleavage along the peptide backbone, yielding an a_3 ion as the most abundant peak in the spectrum. A minor a_5 fragment is also observed, in

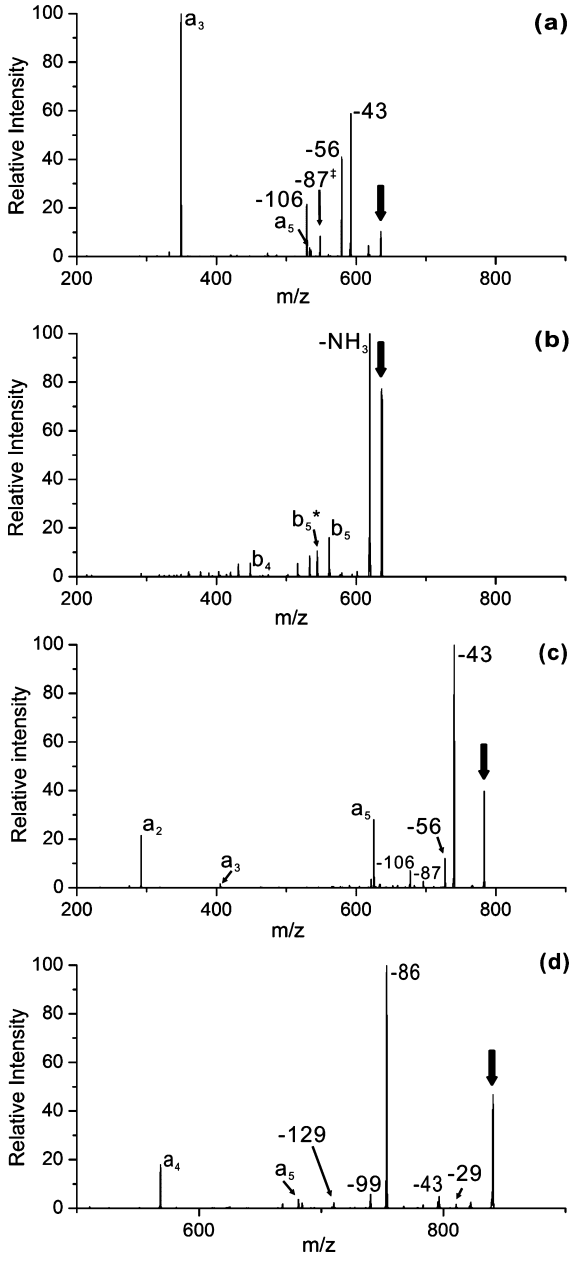

Figure 2. (a) Fragmentation of $[RGYALG\cdot + H]^+$ results in backbone cleavage at tyrosine. (b) By comparison, CID is dominated by loss of NH_3. (c) Fragmentation of $[RYLGYL\cdot + H]^+$ also results in backbone fragmentation at tyrosine. (d) Fragmentation of $[RRPWIL\cdot + H]^+$ yields backbone dissociation at tryptophan. Bold down arrows indicate ions subject to activation. (‡) This peak results from consecutive losses of 43 and 44; (*) loss of NH_3.

addition to several side chain losses. For comparison, the CID spectrum for the protonated peptide is shown in Figure 2b. Following CID, the loss of ammonia dominates and few backbone fragments are observed. No backbone dissociation at Tyr3 is detected. In fact, there is very little overlap between any of the fragments observed in the two spectra. This suggests that the radical is an active (and perhaps dominant) participant in the chemistry yielding the fragments in Figure 2a. The observation of a-type ions in this spectrum is consistent with previous experiments involving radicals.[12,28] The loss of 106 Da corresponds to elimination of the tyrosine side chain, which has also been observed previously.[3,29] In addition, there are two side chain losses from leucine, corresponding to the loss of 43 and 56 Da. The importance of these losses will be discussed further below.

Following the observation of preferential cleavage at tyrosine, it was hypothesized that aromatic residues might facilitate backbone fragmentation. This possibility was explored further with the peptides RYLGYL and RRPWIL. Fragmentation of $[RYLGYL\cdot + H]^+$ is shown in Figure 2c. For this peptide, abundant backbone fragmentation occurs at both tyrosine residues yielding dominant a_2 and a_5 fragments, confirming that tyrosine does facilitate backbone fragmentation. In addition, modest backbone dissociation at leucine yielding an a_3 ion is observed (this fragment is reminiscent of the a_5 fragment at leucine in Figure 2a). Importantly, no other backbone fragmentations are observed. Side chain losses similar to those in Figure 2a are noted, although the relative intensities are substantially different. $[RRPWIL\cdot + H]^+$ which contains tryptophan, was fragmented as shown in Figure 2d. Again, a single dominant backbone fragment corresponding to cleavage at the tryptophan residue to yield an a_4 ion is observed. The only other backbone cleavage is minor and occurs at isoleucine to yield an a_5 fragment. Interestingly, arginine side chain loss (−86 Da) is prevalent for this peptide, which was not observed previously despite the presence of arginine in the previous two peptides (RGYALG and RYLGYL). In addition, there are minor peaks corresponding to the loss of side chains from leucine, isoleucine, and tryptophan.

The fragmentation spectrum for bradykinin $[RPPGFSPFR\cdot + 2H]^{2+}$, which contains two phenylalanines, is shown in Figure 3a. There are two dominant a-type fragments, a_5 and a_8, which correspond to cleavage at the phenylalanine residues. This confirms that aromatic residues facilitate fragmentation of the peptide backbone in general. Complete examination of the spectrum reveals that minor a-type fragments are also observed at Pro2 and Ser6. There is also a novel cleavage between phenylalanine and serine, yielding c_5 and z_4 ions. This observation relates to the presence of serine as is discussed further below. In addition, side chain losses from arginine are prominent, and several low intensity y-type ions are observed. Some of the y ions are radicals. The results from bradykinin suggest that increased sequence diversity can lead to a larger number of fragmentation pathways; however, comparison with the CID spectrum for the nonradical peptide (see Supporting Information) reveals small overlap suggesting that most of the fragments are generated by radical chemistry.

The spectrum shown in Figure 3b illustrates fragmentation of radical angiotensin II, $[DRVYIHPF\cdot + 2H]^{2+}$. In this case, an extensive series of a-type fragments is observed. Comparison with CID of $[DRVYIHPF + 2H]^{2+}$ reveals that a-type ions are not generated in abundance by collisional activation in the absence of a radical (please see Supporting Information). Fragmentation at Tyr4 to yield a_4 is favorable and yields the largest backbone fragment. Abundant a_3 and a_6 ions, corresponding to cleavage at Val3 and His6 are also observed. Minor a_5 and a_7 ions are produced as well. Overall, the dominant fragmentation channels for this peptide are side chain losses from tyrosine (−106) and aspartic acid (−44). The loss of CO_2 could also theoretically occur from the C-terminus, but CID of the −44 fragment confirms that this loss occurs primarily from aspartic acid (please see Supporting Information). The loss of CO_2 has been observed almost exclusively in previous experiments utilizing photoactivation of benzophenone.[30]

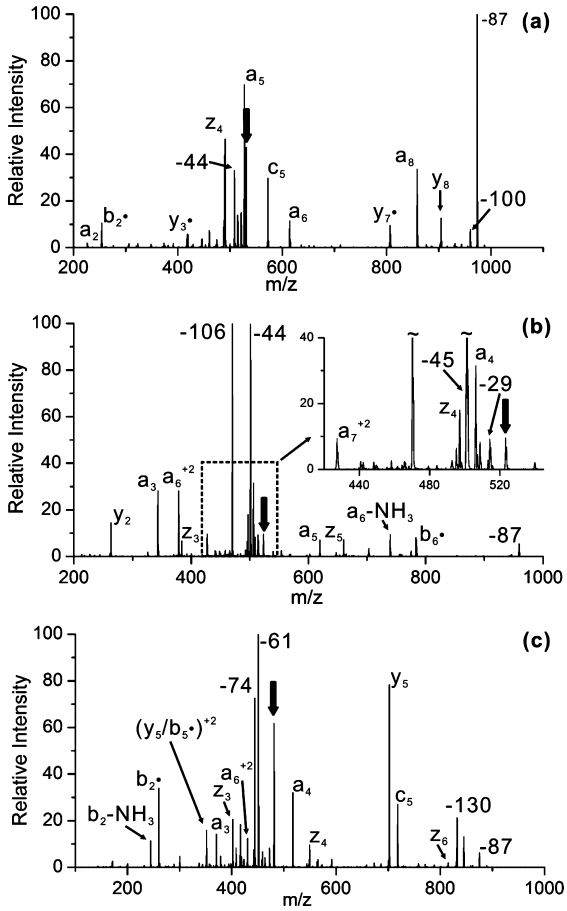

Figure 3. (a) Fragmentation of $[RPPGFSPFR\cdot + 2H]^{2+}$ yields several fragments, including abundant fragmentation at both phenylalanine residues. (b) Fragmentation of $[DRVYIHPF\cdot + 2H]^{2+}$. A nearly complete series of a-type ions is observed. (c) Fragmentation of $[MEHFRWG\cdot + 2H]^{2+}$. Abundant side chain losses at methionine and several backbone fragments are observed.

The results for fragmenting $[MEHFRWG\cdot + 2H]^{2+}$ are shown in Figure 3c. This peptide contains several aromatic residues and methionine. As expected due to the presence of sulfur, fragmentation of the methionine side chain is favorable, yielding intense losses of 61 and 74. Atypically, there is also an abundant y_5 ion. This fragment is also dominant in the CID spectrum of the nonradical peptide indicating that cleavage of EH peptide bond is facile and not initiated by a radical. Significant a-type fragments are generated at Phe4 and Trp6, in agreement with previous results. In addition, fragmentation at His3 yields an abundant a_3 ion. There are also several z-type ions, which are discussed in greater detail below. In general, the fragmentation of this peptide follows similar trends to those observed in previous examples above.

Backbone Fragmentation. Backbone dissociation to yield a-type fragments occurs primarily following abstraction of a β-hydrogen as shown in Scheme 1. Consequently, a-type ions are never generated at glycine. Furthermore, the charge does not participate or affect the reaction and is assumed to be sequestered elsewhere. A similar pathway can also lead to the generation of c- and z-type ions, but this pathway is usually kinetically disfavored by several orders of magnitude according to theory.[31] Experimentally, we have determined that fragmentation at serine and threonine are the only exceptions. These

Scheme 1

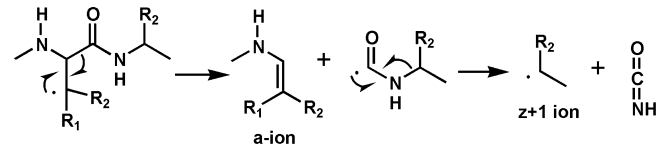

residues generate c and z ions (please see Supporting Information). Importantly, regardless of whether c and z or a and x ions are produced, backbone fragmentation is mediated by initial abstraction of the β-hydrogen for all residues (except glycine).

The nature of the z ions observed in these experiments requires further clarification. Most of the z ions assigned herein are actually z + 1 ions (the same z-ion typically observed in ECD); however, true z ions would be generated by β-scission.[8] The presumed origin for most of the z + 1 ions relates to the x-type fragments from Scheme 1. The x-type ions shown in Scheme 1 are unstable radical species which are never directly observed. However, it is possible for the x-ion to be stabilized by loss of isocyanic acid, yielding a z + 1 ion. Indeed, there are several z + 1 ions that are the complement ions to the abundant a-type fragments present in Figure 3. Nevertheless, z + 1 ions are not always observed and are typically found in small abundance. One explanation for this is that an alternate pathway proceeding by loss of CO followed by loss of the proximate residue can yield an x_{n-1} radical fragment. This route can be repeated indefinitely and possibly lead to degradation of the entire C-terminal radical fragment.

Close examination of the results presented thus far reveals that backbone fragmentation appears to be favored at certain residues, as is most clearly illustrated in the case of aromatic side chains. Is there a rationale which can be used to account for this behavior? Selective fragmentation can only occur if some reaction routes are more favorable than others. For backbone fragmentation, selectivity should result if the initial β-radical in Scheme 1 is preferentially formed at particular amino acids. To understand how this occurs, both the kinetics and dynamics of the reactions leading to the formation of these radicals must be examined. The kinetics are relatively straightforward, where barriers to hydrogen abstraction in amino acids have been calculated, they are small or nonexistent in the absence of conformational barriers.[32–34] Conformational restraint can introduce barriers.[35] Therefore, if a reaction is thermodynamically favorable and the reactants can be brought together without steric hindrance, it should proceed spontaneously. Comparison of the thermodynamics is easily afforded by calculating the BDEs for removing hydrogen from each of the relevant species. The BDE for the α-naphthyl hydrogen is approximately 475 kJ/mol,[36] which is quite large and should enable the naphthyl radical to abstract hydrogen from virtually every site in a peptide. Indiscriminate reactivity is usually not a recipe for selectivity!

The key to understanding the results is that, following the initial hydrogen abstraction, the next thermodynamically favored reaction can also proceed without barrier. In this manner, the radical site can "flow" downhill to a thermodynamically favored location, assuming that conformational flexibility of the peptide allows interaction between the relevant reaction sites. The calculated BDE values for abstracting the α- and β-hydrogens from all of the amino acids are shown in Figure 4 along with estimated uncertainties. The α-hydrogens are always easier

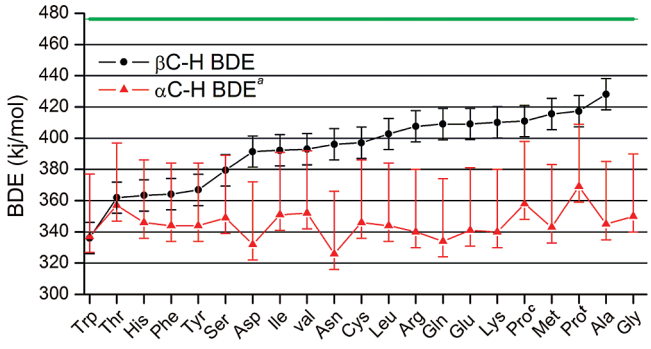

Figure 4. The calculated α and *β* BDEs for each amino acid are shown. The horizontal green line indicates the BDE for naphthalene. The trend for lower BDE in aromatic residues correlates well with the observation of more intense backbone fragmentation. See text for discussion. (a) α BDEs taken from ref 21; c, cis; t, trans.

to abstract due to captodative stabilization; however, the BDEs for α-hydrogens and the magnitude of the captodative effect are very sensitive to peptide structure.[37] If the nascent radical cannot adopt a planar configuration or favorable dihedral angles, the BDE can increase by as much as 40 kJ/mol.[21] Structural effects can therefore cause the α and *β* BDEs to overlap for the lower *β* BDEs. Indeed, the aromatic residues which have the lowest *β* BDEs and should be among the most competitive sites for *β*-radical formation are experimentally observed to be the most favored sites for backbone dissociation. In contrast, amino acids with high *β* BDEs, such as methionine or alanine, never yield abundant a-type ions. In simplified terms, the amino acids on the left side of Figure 4 will yield both side chain and backbone fragments, while the amino acids on the right side will primarily produce side chain losses. The relative intensity of backbone fragments is also frequently correlated with position in Figure 4, with those amino acids more to the left yielding more abundant backbone fragments. For example, the relative intensities of the a-type ions in Figure 2 follow the predicted trends, with fragments at tyrosine or tryptophan being favored over those at leucine or isoleucine.

Very importantly, the magnitudes of the *β* BDEs themselves are dictated by side chain composition, meaning that fragmentation of the peptide backbone in these experiments is controlled primarily by side chain chemistry. This contrasts sharply with other currently available dissociation methods. CID fragmentation is controlled largely by the presence or absence of mobile protons.[38] The influence of side chains is highly variable in CID fragmentation. For example, the hydrocarbon side chains (alanine, valine, leucine, isoleucine, phenylalanine) have little influence on CID, yet fragmentation at these residues can occur. On the other hand, aspartic acid and proline actually facilitate backbone cleavage, but fragmentation does not always occur at these residues for all peptides.[39,40] In the final analysis, CID can only be predicted with bioinformatic approaches, and even then prediction is difficult and will be dependent on the overlap between training and data sets.[41] Fragmentation of the backbone by ECD and ETD is well-known to occur without regard for side chains or even post-translational modifications.[42] The fact that radical mediated fragmentation yields primarily a-type ions where the abundance of each backbone cleavage is correlated with side chain composition is unique and should enable greater predictability of the results.

Side Chain Losses. It is clear from the experimental data that side chain losses play an important role in the chemistry

Scheme 2

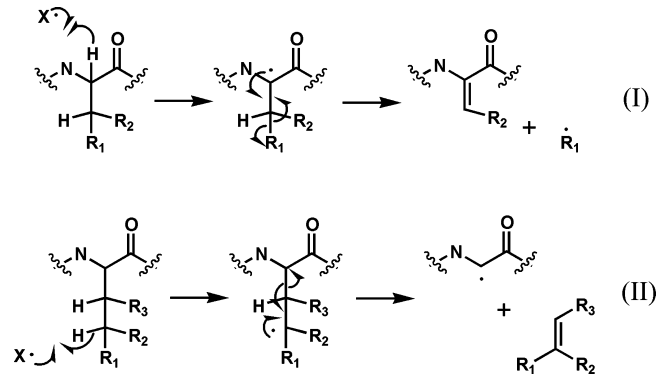

Table 1. Side Chain Loss Masses by Mechanism

	side chain losses			
amino acids	I	II	III[a]	IV[b]
Ala[c]	--	--		
Arg	86, 87[d]	99, 100[d]		72
Asn	44	--		
Asp	45	--		44
Cys	33	46		
Glu	59	72		45, 44
Gln	58	71		
Gly	--	--		
His	67	--	80	
Ile	29	56		
Leu	43	56		
Lys	58, 59[d]	71, 72[d]		
Met	61	74		47
Phe	*77*	--		
Pro	--	--		
Ser	17[e]	30		
Thr	15[e]	44		
Trp	116[e]	--	129, 130[d]	
Tyr	93[e]	--	106	
Val	*15*	*42*		

[a] Diverse mechanisms which yield the same peptide fragment as in (II). [b] Various other experimentally observed side chain losses. [c] Amino acids in italics do not exhibit any substantial side chain losses. [d] These losses are protonated side chains. [e] Never observed.

of radical peptide dissociation. Previous experiments have demonstrated that similar side chains losses can occur in ECD experiments.[43] In contrast to backbone fragmentation, side chain losses are initiated by a diverse set of pathways.[44] Perhaps the two most common pathways are shown in Scheme 2 (again charges do not play an appreciable role and are not explicitly shown). Mechanism (I) illustrates abstraction of the α-hydrogen to generate dehydroalanine, which leads to loss of a radical side chain fragment. Abstraction of the *γ*-hydrogen, as shown in mechanism (II), leaves the radical on the peptide in the α-position following loss of the entire side chain. Other mechanisms can mimic the results produced by (II). For example, abstraction of the tyrosine side chain -OH hydrogen followed by electronic rearrangement and loss of *p*-quinomethide yields the same peptide product as would be generated by (II). The predicted and observed side chain losses for all amino acids are shown below in Table 1. Data interpretation is somewhat simplified by the fact that not all amino acids will exhibit side chain losses. For example, glycine has no side chain. Alanine and proline cannot lose a side chain by mechanisms (I) or (II) and are not predicted to lose a side chain by any other energetically competitive route. Phenylalanine and

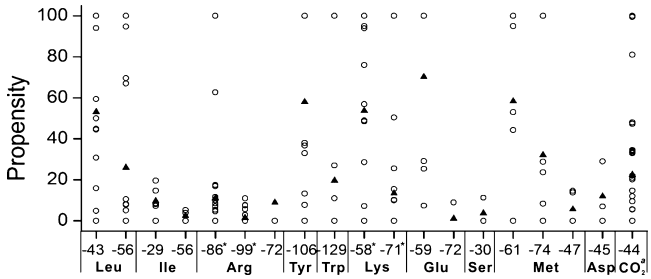

Figure 5. Propensities for side chain losses at each amino acid are given by mass. The propensities do not follow obvious trends and frequently fill the entire scale. Average values for each column are indicated by black triangles. (a) Loss from Glu, Asp, and the C-terminus; (*) protonated or neutral losses.

valine side chain loss by either mechanism is unlikely because aromatic or primary carbon radicals are involved. In fact, side chains losses are not observed for glycine, alanine, proline, phenylalanine, or valine to any significant extent. Thus, one-quarter of amino acids are typically not subject to side chain losses.

The propensity for observing each side chain loss from a collection of peptides is shown along with the average values in Figure 5. The propensity for a loss is defined as the abundance of a loss relative to the largest side chain loss divided by the number of times that amino acid occurs in the peptide. If no side chain loss for an amino acid in a peptide which contains that amino acid is observed, the propensity is zero. The maximum value would be 100 for the most abundant side chain loss observed in a peptide with only one occurrence of that amino acid. For several amino acids, the propensity for side chain loss ranges from 0 to 100, covering the entire range of possible values. The propensities are fairly scattered in general. This indicates that neither the occurrence nor relative intensity of side chain losses are easily predictable for a given peptide of unknown sequence. This may relate to the variety of pathways which lead to side chain losses. Consideration of the average propensities (shown in dark triangles) is more revealing. For each amino acid, the average loss from mechanism (I) occurs in greater abundance than the average loss from mechanism (II). This trend is in perfect agreement with the results that would be expected based on the relative BDEs shown in Figure 4. Furthermore, it is clear that (on average) some side chains are more reactive than others. One striking example is the greater fragmentation propensity of leucine compared to isoleucine.

Utility of Side Chains Losses. Despite the fact that side chain losses are unpredictable, they are easily identified and can still yield important information. For example, leucine and isoleucine can be distinguished by side chain losses because unique mass fragments are generated by mechanism (II).[45] Furthermore, any unique mass side chain loss positively identifies one amino acid in the peptide (although its location is obviously not revealed). There are 11 amino acids which can be uniquely identified by side chain loss. The remaining 4 amino acids can be narrowed down to 2 or 3 possibilities. Because of the infrequency for which complete series backbone fragments are generated by CID, the identities of many amino acids in a peptide are not directly available. Of the amino acids in the peptides studied presently, side chain losses led to the positive identification of amino acids for 10/15 of the peptides for which the identity was not apparent from backbone dissociations.

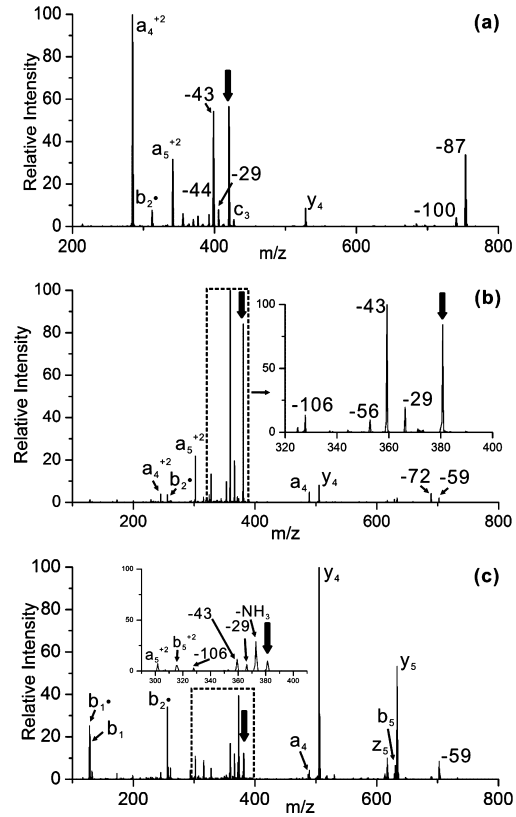

Figure 6. (a) Fragmentation of $[RRPWIL^{\bullet} + 2H]^{2+}$ yields a spectrum similar to the singly protonated radical. (b) Fragmentation of $[KKPYIL^{\bullet} + 2H]^{2+}$ prepared from [KKPYIL + **2** + 3H]$^{3+}$ revealing a typical spectrum. (c) Fragmentation of $[KKPYIL^{\bullet} + 2H]^{2+}$ prepared from [KKPYIL + **2** + 2H]$^{2+}$ yields a very dissimilar spectrum, revealing the influence of structural effects. This peptide is unique in this behavior.

When submitting MS/MS information to a database, any hits not containing these amino acids could be eliminated.

Influence of Charge State. Charge state does not typically play a dominant role in the fragmentation observed for the radical peptides herein. For example, doubly protonated $[RRPWIL^{\bullet} + 2H]^{2+}$ yields the fragmentation spectrum shown in Figure 6a. For the most part, similar fragments are generated as those observed in Figure 2d for the singly protonated peptide. The primary difference between the spectra is that the relative intensities of several fragments change significantly. Interestingly, the a_4 ion becomes the base peak and arginine side chain loss is suppressed. Also interesting is the increased abundance of the loss of leucine side chain (−43). The relative intensities of the a-type fragments with respect to each other have not changed, which is consistent with our description of backbone fragmentation above. Overall, these results suggest again that fragmentation is primarily controlled by radical rather than charge directed processes, in agreement with previous findings examining energetics explicitly.[27]

One situation where charge state can play a significant role is when a single charge is sequestered by the C-terminal portion of the peptide. This is demonstrated by the fragmentation of $[MEHFRWG^{\bullet} + H]^{+}$ (please see Supporting Information), which generates fewer backbone fragments than $[MEHFRWG^{\bullet} + 2H]^{2+}$. This is most likely due to the fact that the singly protonated molecule will be preferentially charged at arginine, preventing observation of a-type fragments smaller than a_5. To

avoid this situation, higher charge states should be interrogated when multiple options exist.

Influence of Peptide Structure. For the majority of peptides examined, the three-dimensional structure (although presumed to be present) does not significantly influence backbone dissociation. However, we did encounter one striking example to the contrary. The peptide $[KKPYIL\cdot + 2H]^{2+}$ yields a typical dissociation spectrum when generated from the +3 noncovalent complex as shown in Figure 6b. In this case, the crown departs with a charge following hydrogen abstraction, yielding the doubly protonated peptide radical. The results contrast sharply with what happens when the +2 radical peptide is generated from the doubly charged noncovalent complex as shown in Figure 4c. In this case, b and y ions dominate the spectrum. Radical initiated fragments are also present, but the relative intensities have changed dramatically between Figure 6b and 6c for fragmentation of the same ion! The most likely explanation in this case is that the +2 complex is situated such that the initial radical site on the peptide is already stable and does not migrate to other locations. This leads to abundant fragments that are similar to CID of the nonradical (please see Supporting Information), In fact, assignment of these peaks localizes the radical to the first two residues, as the fragments containing these amino acids are radicals. The +3 complex will undoubtedly have a different and probably more extended structure, making it unlikely that the original site of abstraction is the same. This is the only peptide which is observed to behave this way. The preparation of the ion did not greatly affect the results for the other peptides (not all can be prepared by multiple paths). Briefly, structure can affect the results, but most of the time this will be manifested in variations in relative intensity rather than in the appearance or absence of fragments.

Radical Transfer. Side chain losses can also be used to explore the possibility for radical transfer or migration.[35] The spectra shown in Figure 7 illustrate what happens when several of the side chain losses in Figure 2a were reisolated and subjected to further collisional activation. In Figure 7a, the product resulting from tyrosine side chain loss was subjected to CID. Loss of the tyrosine side chain leaves the radical initially on the α-carbon. As shown in Figure 7a, activation of this radical leads to dominant side chain losses from leucine. Minor loss of CO_2 is also observed in conjunction with other losses. Fragmentation of the backbone to yield the $a_5 - 106$ peak represents a minor dissociation channel. In the absence of more competitive dissociation pathways, fragmentation at Ala4 to yield the $a_4 - 106$ ion is even observed in very minor abundance. These results suggest that radical movement is primarily in the thermodynamically favored direction, as discussed above. In Figure 7b the peak corresponding to the −56 Da leucine side chain loss, which will again generate a radical on the α-carbon, is subjected to further collisional activation. Interestingly, the a_3 ion is by far the most abundant fragment that is generated, followed by the loss of CO_2 and tyrosine side chain. This confirms that following radical migration to an α position, abstraction of a β-hydrogen from an aromatic residue is still a facile process. Furthermore, no appreciable fragmentation at Ala4 is observed, as was the case in Figure 7a. Abstraction of the β-hydrogen from alanine is simply not competitive in the presence of tyrosine, again in agreement with the predicted chemistry. In Figure 7c, further activation of the −43 Da leucine side chain loss is shown. In this situation, a radical fragment is lost, meaning that the peptide is not a radical. Although the spectrum in Figure 7c does contain some a-type fragments not observed in the CID spectrum for the protonated peptide (see Figure 2b), in general, fragmentation is similar in both spectra.

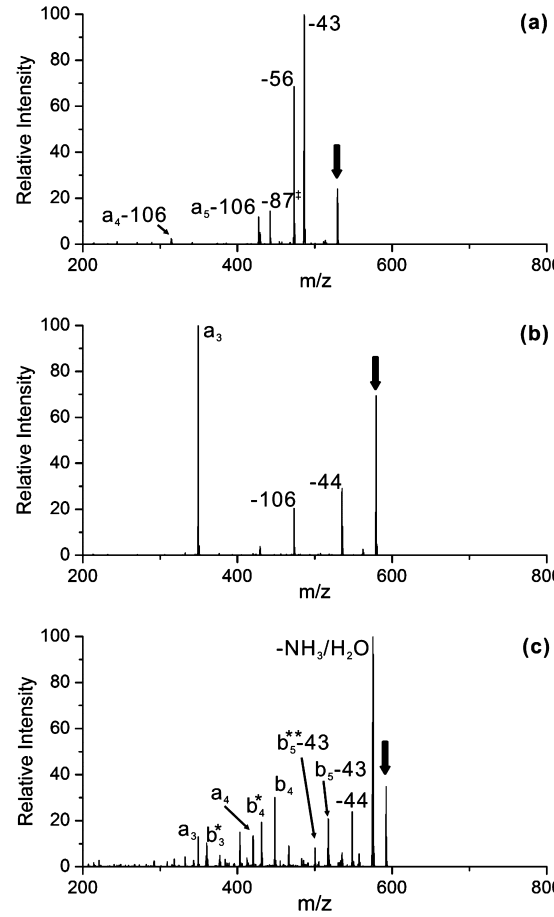

Figure 7. The side chain losses observed in Figure 2a are reisolated and subjected to further collisional activation. Radical migration can be monitored. The relative energetics of different mechanistic pathways can be compared from a known starting point. (a) CID spectrum for $[RGYALG\cdot - 106 + H]^+$. (b) CID spectrum for $[RGYALG\cdot - 56 + H]^+$.c) CID spectrum for $[RGYALG\cdot - 43 + H]^+$. (*) Loss of NH_3; (**) loss of H_2O; (‡) consecutive loss of 44 and 43.

These results demonstrate that radical migration is possible. For example, if the initially formed naphthyl radical abstracts the α-hydrogen from leucine in RGYALG, then it is clear that this radical can in turn abstract a hydrogen atom from the β position of tyrosine to yield the a_3 fragment. Similarly, it is likely that abstraction of the hydrogens from either glycine residue could lead to a similar outcome. The probability for subsequent abstractions relates to the relevant barriers. For example, abstraction of the leucine α-hydrogen could also be followed by side chain loss; however, if this channel is guarded by a larger barrier, then abstraction of the β-hydrogen of tyrosine may prevail. The results also suggest that peptides are sufficiently flexible to minimize any conformational barriers which might prevent radical migration.

Conclusions

We have demonstrated that hydrogen deficient peptide radicals can be easily generated by the noncovalent attachment of a suitable photolabile hydrogen abstraction reagent. Collisional activation of these hydrogen deficient peptide radicals

yields fragmentation patterns which are dissimilar to those produced by CID of nonradical peptides, ECD, ETD, or related techniques. It is found that radical chemistry controls the preferred fragmentation pathways, and that all other factors such as mobile protons or peptide structure play a secondary role. Interestingly, backbone fragmentation produces primarily a-type ions, and the probability for dissociation is dictated by the nature of the side chains to a greater extent than is observed with any other fragmentation method. This should translate into greater predictability of the results, and subsequently greater confidence in data analysis tasks such as peptide identification. Verification of this hypothesis will require analysis of a larger set of peptides, which is currently limited by the need for a more efficient method of preparing the peptide radicals. Fortunately, there are many available remaining options that have not been fully explored.

In addition to interesting backbone fragmentations, numerous side chain losses are observed. It is demonstrated that a large number of these losses can be used to uniquely identify amino acids in a peptide. Although the location of the amino acid is not revealed, this information can be used to narrow down candidate peptides during a database search. All peptides not containing the amino acids identified by side chain losses are simply eliminated from the search. The orthogonality and potential utility of the data obtained by fragmenting hydrogen deficient radical peptides relative to other fragmentation techniques merits further exploration of this methodology.

Relative to most charge directed pathways, radical chemistry is able to dominate the fragmentation of peptides in these experiments by lowering the barriers to dissociation. In this regard, photoactivation is important for radical generation because the entire molecule is not heated substantially in the process. Although collisional activation can be easily implemented for radical activation, the concomitant heating of the entire peptide can also enable nonradical dissociation pathways or less favorable radical dissociation pathways. This situation will be particularly acute if the barrier to generate the radical is substantial and larger than subsequent fragmentation barriers (which would be predicted to be the case since radicals typically facilitate fragmentation). Furthermore, mobile protons can prevent or interfere with radical generation by collisional activation but are not observed to affect photoactivation. Although our results are largely similar to those produced previously with collisionally activated radicals, we observe less fragmentation overall which we attribute to cooler radical generation.

Acknowledgment. The authors thank the National Science Foundation for funding (CHE-0747481 for R.R.J.). H.N. thanks the Ford Foundation for a predoctoral scholarship. B.M.S. and H.N. thank Caltech for funding.

Supporting Information Available: Additional mass spectra and the mechanism for c and z formation. This material is available free of charge via the Internet at http://pubs.acs.org.

References

(1) Zubarev, R. A.; Horn, D. M.; Fridriksson, E. K.; Kelleher, N. L.; Kruger, N. A.; Lewis, M. A.; Carpenter, B. K.; McLafferty, F. W. *Anal. Chem.* **2000**, *72*, 563–573.
(2) Syka, J. E. P.; Coon, J. J.; Schroeder, M. J.; Shabanowitz, J.; Hunt, D. F. *Proc. Natl. Acad. Sci. U.S.A.* **2004**, *101*, 9528–9533.
(3) Chu, I. K.; Rodriquez, C. F.; Lau, T. C.; Hopkinson, A. C.; Siu, K. W. M. *J. Chem. Phys. B* **2000**, *104*, 3393–3397.
(4) Wee, S.; O'Hair, R. A. J.; McFadyen, W. D. *Int. J. Mass Spectrom.* **2004**, *234*, 101–122.
(5) Bagheri-Majdi, E.; Ke, Y. Y.; Orlova, G.; Chu, I. K.; Hopkinson, A. C.; Siu, K. W. M. *J. Chem. Phys. B* **2004**, *108*, 11170–11181.
(6) Barlow, C. K.; Wee, S.; McFadyen, W. D.; O'Hair, R. A. J. *Dalton Trans.* **2004**, 3199–3204.
(7) Laskin, J.; Yang, Z.; Chu, I. K. *J. Am. Chem. Soc.* **2008**, *130*, 3218–3230.
(8) Hodyss, R.; Cox, H. A.; Beauchamp, J. L. *J. Am. Chem. Soc.* **2005**, *127*, 12436–12437.
(9) Hao, G.; Gross, S. S. *J. Am. Soc. Mass Spectrom.* **2006**, *17*, 1725–1730.
(10) Yin, H.; Chacon, A.; Porter, N. A.; Yin, H. Y.; Masterson, D. S. *J. Am. Soc. Mass Spectrom.* **2007**, *18*, 807–816.
(11) Masterson, D. S.; Yin, H. Y.; Chacon, A.; Hachey, D. L.; Norris, J. L.; Porter, N. A. *J. Am. Chem. Soc.* **2004**, *126*, 720–721.
(12) Ly, T.; Julian, R. R. *J. Am. Chem. Soc.* **2008**, *130*, 351–358.
(13) Diedrich, J. K.; Julian, R. R. *J. Am. Chem. Soc.* **2008**, *130*, 12212–12213.
(14) Julian, R. R.; May, J. A.; Stoltz, B. M.; Beauchamp, J. L. *Ang. Chem., Int. Ed.* **2003**, *42*, 1012–1015.
(15) Julian, R. R.; Beauchamp, J. L. *J. Am. Soc. Mass Spectrom.* **2004**, *15*, 616–624.
(16) Friess, S. D.; Daniel, J. M.; Hartmann, R.; Zenobi, R. *Int. J. Mass Spectrom.* **2002**, *219*, 269–281.
(17) Julian, R. R.; Akin, M.; May, J. A.; Stoltz, B. M.; Beauchamp, J. L. *Int. J. Mass Spectrom.* **2002**, *220*, 87–96.
(18) Julian, R. R.; Beauchamp, J. L. *Int. J. Mass Spectrom.* **2001**, *210*, 613–623.
(19) Wilson, J. J.; Kirkovits, G. J.; Sessler, J. L.; Brodbelt, J. S. *J. Am. Soc. Mass Spectrom.* **2008**, *19*, 257–260.
(20) Jemmett, A. E.; Tucker, S. H.; Wellings, I. *J. Chem. Soc.* **1958**, 2794–2797.
(21) Rauk, A.; Yu, D.; Taylor, J.; Shustov, G. V.; Block, D. A.; Armstrong, D. A. *Biochemistry* **1999**, *38*, 9089–9096.
(22) Armstrong, D. A.; Yu, D.; Rauk, A. *Can. J. Chem.* **1996**, *74*, 1192–1199.
(23) Blanksby, S. J.; Ellison, G. B. *Acc. Chem. Res* **2003**, *36*, 255–263.
(24) Rauk, A.; Yu, D.; Armstrong, D. A. *J. Am. Chem. Soc.* **1997**, *119*, 208–217.
(25) NIST Computational Chemistry Comparison and Benchmark Database, NIST Standard Reference Database Number 101 Release 14, September 2006; Russell D. Johnson, III, Ed. http://srdata.nist.gov/cccbdb.
(26) Kavita, K.; Das, P. K. *J. Chem. Phys.* **2002**, *117*, 2038–2044.
(27) Nielsen, M. L.; Budnik, B. A.; Haselmann, K. F.; Olsen, J. V.; Zubarev, R. A. *Chem. Phys. Lett.* **2000**, *330* (5−6), 558–562.
(28) Laskin, J.; Yang, Z. B.; Lam, C.; Chu, I. K. *Anal. Chem.* **2007**, *79*, 6607–6614.
(29) Barlow, C. K.; McFadyen, W. D.; O'Hair, R. A. J. *J. Am. Chem. Soc.* **2005**, *127*, 6109–6115.
(30) Bossio, R. E.; Hudgins, R. R.; Marshall, A. G. *J. Phys.Chem. B* **2003**, *107*, 3284–3289.
(31) Wood, G. P. F.; Easton, C. J.; Rauk, A.; Davies, M. J.; Radom, L. *J. Phys. Chem. A* **2006**, *110*, 10316–10323.
(32) Galano, A.; Alvarez-Idaboy, J. R.; Bravo-Perez, G.; Ruiz-Santoyo, M. E. *J. Mol. Struct.: THEOCHEM* **2002**, *617*, 77–86.
(33) Galano, A.; Alvarez-Idaboy, J. R.; Agacino-Valdes, E.; Ruiz-Santoyo, M. E. *J. Mol. Struct.: THEOCHEM* **2004**, *676*, 97–103.
(34) Cruz-Torres, A.; Galano, A.; Alvarez-Idaboy, J. R. *Phys. Chem. Chem. Phys.* **2006**, *8*, 285–292.
(35) Chu, I. K.; Zhao, J.; Xu, M.; Siu, S. O.; Hopkinson, A. C.; Siu, K. W. M. *J. Am. Chem. Soc.* **2008**, *130*, 7862–7872.
(36) Lardin, H. A.; Squires, R. R.; Wenthold, P. G. *J. Mass Spectrom.* **2001**, *36*, 607–615.
(37) Rauk, A.; Yu, D.; Armstrong, D. A. *J. Am. Chem. Soc.* **1997**, *119* (1), 208–217.
(38) Dongre, A. R.; Jones, J. L.; Somogyi, A.; Wysocki, V. H. *J. Am. Chem. Soc.* **1996**, *118*, 8365–8374.
(39) Loo, J. A.; Edmonds, C. G.; Smith, R. D. *Anal. Chem.* **1993**, *65*, 425–438.
(40) Tsaprailis, G.; Somogyi, A.; Nikolaev, E. N.; Wysocki, V. H. *Int. J. Mass Spectrom.* **2000**, *196*, 467–479.
(41) Zhang, Z. Q. *Anal. Chem.* **2004**, *76*, 3908–3922.
(42) Sweet, S. M. M.; Cooper, H. J. *Expert Rev. Proteomics* **2007**, *4*, 149–159.
(43) Fung, Y. M. E.; Chan, T. W. D. *J. Am. Soc. Mass Spectrom.* **2005**, *16*, 1523–1535.
(44) Barlow, C. K.; McFadyen, W. D.; O'Hair, R. A. J. *J. Am. Chem. Soc.* **2005**, *127*, 6109–6115.
(45) Wee, S.; O'Hair, R. A. J.; McFadyen, W. D. *Rapid Commun. Mass Spectrom.* **2002**, *16*, 884–890.

PR800592T